A&A 470, 721–726 (2007)
DOI: 10.1051/0004-6361:20077361

Astronomy & Astrophysics

The HARPS search for southern extra-solar planets

IX. Exoplanets orbiting HD 100777, HD 190647, and HD 221287⋆,⋆⋆

D. Naef[1,2], M. Mayor[2], W. Benz[3], F. Bouchy[4], G. Lo Curto[1], C. Lovis[2], C. Moutou[5], F. Pepe[2], D. Queloz[2], N. C. Santos[2,6,7], and S. Udry[2]

[1] European Southern Observatory, Casilla 19001, Santiago 19, Chile
e-mail: dnaef@eso.org
[2] Observatoire de Genève, Université de Genève, 51 Ch. des Maillettes, 1290 Sauverny, Switzerland
[3] Physikalisches Institut Universität Bern, Sidlerstrasse 5, 3012 Bern, Switzerland
[4] Institut d'Astrophysique de Paris, UMR7095, Université Pierre & Marie Curie, 98bis Bd Arago, 75014 Paris, France
[5] Laboratoire d'Astrophysique de Marseille, Traverse du Siphon, 13376 Marseille 12, France
[6] Centro de Astronomia e Astrofísica da Universidade de Lisboa, Observatório Astronómico de Lisboa, Tapada da Ajuda, 1349-018 Lisboa, Portugal
[7] Centro de Geofísica de Évora, Rua Romão Ramalho 59, 7002-554 Évora, Portugal

Received 26 February 2007 / Accepted 11 April 2007

ABSTRACT

Context. The HARPS high-resolution high-accuracy spectrograph was made available to the astronomical community in the second half of 2003. Since then, we have been using this instrument for monitoring radial velocities of a large sample of Solar-type stars (≃1400 stars) in order to search for their possible low-mass companions.
Aims. Amongst the goals of our survey, one is to significantly increase the number of detected extra-solar planets in a volume-limited sample to improve our knowledge of their orbital elements distributions and thus obtain better constraints for planet-formation models.
Methods. Radial-velocities were obtained from high-resolution HARPS spectra via the cross-correlation method. We then searched for Keplerian signals in the obtained radial-velocity data sets. Finally, companions orbiting our sample stars were characterised using the fitted orbital parameters.
Results. In this paper, we present the HARPS radial-velocity data and orbital solutions for 3 Solar-type stars: HD 100777, HD 190647, and HD 221287. The radial-velocity data of HD 100777 is best explained by the presence of a 1.16 $M_{\rm Jup}$ planetary companion on a 384-day eccentric orbit (e = 0.36). The orbital fit obtained for the slightly evolved star HD 190647 reveals the presence of a long-period (P = 1038 d) 1.9 $M_{\rm Jup}$ planetary companion on a moderately eccentric orbit (e = 0.18). HD 221287 is hosting a 3.1 $M_{\rm Jup}$ planet on a 456-day orbit. The shape of this orbit is not very well-constrained because of our non-optimal temporal coverage and because of the presence of abnormally large residuals. We find clues that these large residuals result from spectral line-profile variations probably induced by processes related to stellar activity.

Key words. stars: individual: HD 100777 – stars: individual: HD 190647 – stars: individual: HD 221287 – stars: planetary systems – techniques: radial velocities

1. Introduction

The *High Accuracy Radial-velocity Planet Searcher* (HARPS, Pepe et al. 2002, 2004; Mayor et al. 2003) was put in operation during the second half of 2003. HARPS is a high-resolution, fiber-fed echelle spectrograph mounted on the 3.6-m telescope at ESO-La Silla Observatory (Chile). It is placed in a vacuum vessel and is accurately thermally-controlled (temperature variations are less than 1 mK over one night, less than 2 mK over one month). Its most striking characteristic is its unequaled stability and radial-velocity (RV) accuracy: 1 m s^{-1} in routine operations. A sub-m s^{-1} accuracy can even be achieved for inactive, slowly rotating stars when an optimized observing strategy aimed at averaging out the stellar oscillations signal is applied (Santos et al. 2004a; Lovis et al. 2006).

The HARPS Consortium that manufactured the instrument for ESO has received Guaranteed Time Observations (GTO). The core programme of the HARPS-GTO is a very high RV-precision search for low-mass planets around non-active and slowly rotating Solar-type stars. Another programme carried out by the HARPS-GTO is a lower RV precision planet search. It is a survey of about 850 Solar-type stars at a precision better than 3 m s^{-1}. The sample is a volume-limited complement (up to 57.5 pc) of the CORALIE sample (Udry et al. 2000). The goal of this sub-programme is to obtain improved Jupiter-sized planets orbital elements distributions by substantially increasing the size of the exoplanets sample. Statistically robust orbital elements distributions put strong constraints on the various planet formation scenarios. The total number of extra-solar planets known so far is over 200. Nevertheless, some sub-categories of planets with special characteristics (e.g. hot-Jupiters or very long-period planets)

⋆ Based on observations made with the HARPS instrument on the ESO 3.6-m telescope at the La Silla Observatory (Chile) under the GTO programme ID 072.C-0488.
⋆⋆ Tables 2–4 are only available in electronic form at http://www.aanda.org

are still weakly populated. The need for additional detections thus remains high.

With typical measurement precisions of $2-3\,\mathrm{m\,s^{-1}}$, the HARPS volume-limited programme does not necessarily aim at detecting very low-mass planetary companions, and it is mostly sensitive to planets that are more massive than Saturn. To date, it has already allowed the detection of several short-period planets: HD 330075 b (Pepe et al. 2004), HD 2638 b, HD 27894 b, HD 63454 b (Moutou et al. 2005), and HD 212301 b (Lo Curto et al. 2006).

In this paper, we report the detection of 3 longer-period planetary companions orbiting stars in the volume-limited sample: HD 100777 b, HD 190647 b, and HD 221287 b. In Sect. 2, we describe the characteristics of the 3 host stars. In Sect. 3, we present our HARPS radial-velocity data and the orbital solutions for the 3 targets. In Sect. 3.4, we discuss the origin of the high residuals to the orbital solution for HD 221287. Finally, we summarize our findings in Sect. 4.

2. Stellar characteristics of HD 100777, HD 190647, and HD 221287

The main characteristics of HD 100777, HD 190647, and HD 221287 are listed in Table 1. Spectral types, apparent magnitudes m_V, colour indexes $B-V$, astrometric parallaxes π, and distances d are from the HIPPARCOS Catalogue (ESA 1997). From the same source, we have also retrieved information on the scatter in the photometric measurements and on the goodness of the astrometric fits for the 3 targets. The photometric scatters are low in all cases. HD 190647 is flagged as a constant star. The goodness-of-fit parameters are close to 0 for the 3 stars, indicating that their astrometric data are explained by a single-star model well. Finally, no close-in faint visual companions are reported around these objects in the HIPPARCOS Catalogue.

We performed LTE spectroscopic analyses of high signal-to-noise ratio (SNR) HARPS spectra for the 3 targets following the method described in Santos et al. (2004b). Effective temperatures ($T_{\rm eff}$), gravities ($\log g$), iron abundances ([Fe/H]), and microturbulence velocities ($V_{\rm t}$) indicated in Table 1 result from these analyses. Like most of the planet-hosting stars (Santos et al. 2004b), HD 100777 and HD 190647 have very high iron abundances, more than 1.5 times the solar value, whereas HD 221287 has a nearly solar metal content. Using the spectroscopic effective temperatures and the calibration in Flower (1996), we computed bolometric corrections. Luminosities were obtained from the bolometric corrections and the absolute magnitudes. The low gravity and the high luminosity of HD 190647 indicate that this star is slightly evolved. The other two stars are still on the main sequence. Stellar masses M_* were derived from L, $T_{\rm eff}$, and [Fe/H] using Geneva and Padova evolutionary models (Schaller et al. 1992; Schaerer et al. 1993; Girardi et al. 2000). Values of the projected rotational velocities, $v \sin i$, were derived from the widths of the HARPS cross-correlation functions using a calibration obtained following the method described in Santos et al. (2002, see their Appendix A)[1].

Stellar activity indexes $\log R'_{\rm HK}$ (see the index definition in Noyes et al. 1984) were derived from Ca II K line core reemission measurements on high-SNR HARPS spectra following the method described in Santos et al. (2000). Using these values and the calibration in Noyes et al. (1984), we derived

[1] Using cross-correlation function widths for deriving projected rotational velocities is a method that was first proposed by Benz & Mayor (1981).

Table 1. Observed and inferred stellar characteristics of HD 100777, HD 190647, and HD 221287 (see text for details).

		HD 100777	HD 190647	HD 221287
HIP		56572	99115	116084
Type		K0	G5	F7V
m_V		8.42	7.78	7.82
$B-V$		0.760	0.743	0.513
π	[mas]	18.84 ± 1.14	18.44 ± 1.10	18.91 ± 0.82
d	[pc]	$52.8^{+3.4}_{-3.0}$	$54.2^{+3.4}_{-3.1}$	$52.9^{+2.4}_{-2.2}$
M_V		4.807	4.109	4.203
$B.C.$		−0.119	−0.109	−0.010
L	[$L_\odot$]	1.05	1.98	1.66
$T_{\rm eff}$	[K]	5582 ± 24	5628 ± 20	6304 ± 45
$\log g$	[cgs]	4.39 ± 0.07	4.18 ± 0.05	4.43 ± 0.16
[Fe/H]		0.27 ± 0.03	0.24 ± 0.03	0.03 ± 0.05
$V_{\rm t}$	[$\mathrm{km\,s^{-1}}$]	0.98 ± 0.03	1.06 ± 0.02	1.27 ± 0.12
M_*	[$M_\odot$]	1.0 ± 0.1	1.1 ± 0.1	1.25 ± 0.10
$\log R'_{\rm HK}$		−5.03	−5.09	−4.59
$P_{\rm rot}$	[d]	39 ± 2	39 ± 2	5.0 ± 2
age	[Gyr]	>2	>2	1.3
$v \sin i$	[$\mathrm{km\,s^{-1}}$]	1.8 ± 1.0	2.4 ± 1.0	4.1 ± 1.0

estimates of the rotational periods and stellar ages. The chromospheric ages obtained with this calibration for HD 100777 and HD 190647 are 6.2 and 7.6 Gyr. Pace & Pasquini (2004) have shown that chromospheric ages derived for very low-activity, Solar-type stars were not reliable. This is due to the fact that the chromospheric emission drops rapidly after 1 Gyr and becomes virtually constant after 2 Gyr. For this reason, we have chosen to indicate ages greater than 2 Gyr instead of the calibrated values for these two stars. HD 221287 is much more active and thus younger making its chromospheric age estimate more reliable: 1.3 Gyr. We have also measured the lithium abundance for this target following the method described in Israelian et al. (2004) and again using a high-SNR HARPS spectrum. The measured equivalent width for the Li I λ6707.70 Å line (deblended from the Fe I λ6707.44 Å line) is 66.6 mÅ leading to the following lithium abundance: $\log n(\mathrm{Li}) = 2.98$. Unfortunately, the lithium abundance cannot provide any reliable age constraint in our case. Studies of the lithium abundances of open cluster main sequence stars have shown that $\log n(\mathrm{Li})$ remains constant and equals $\simeq$3 for $T_{\rm eff} = 6300$ K stars older than a few million years (see for example, Sestito & Randich 2005).

From the activity level reported for HD 221287 ($\log R'_{\rm HK} = -4.59$), we can estimate the expected level of activity-induced radial-velocity scatter (i.e. the *jitter*). Using the results obtained by Santos et al. (2000) for stars with similar activity levels and spectral types, the range of expected jitter is between 8 and $20\,\mathrm{m\,s^{-1}}$. A similar study made on a different stellar sample by Wright (2005) gives similar results: an expected jitter of the order of $20\,\mathrm{m\,s^{-1}}$ (from the fit this author presents in his Fig. 4). It has to be noted that both studies contain very few F stars and even fewer high-activity F stars. This results from the stellar sample they have used: planet search samples selected against rapidly-rotating young stars. Their predictions for the expected jitter level are therefore not well-constrained for active F stars. Both HD 100777 and HD 190647 are inactive and slowly rotating. Following the same studies, low jitter values are expected in both cases: $\leq 8\,\mathrm{m\,s^{-1}}$.

Table 5. HARPS orbital solutions for HD 100777, HD 190647, and HD 221287.

		HD 100777	HD 190647	HD 221287
P	[d]	383.7 ± 1.2	1038.1 ± 4.9	$456.1 \pm {}^{+7.7}_{-5.8}$
T	[JD†]	456.2 ± 2.3	869 ± 24	$263 \pm {}^{+99}_{-52}$
e		0.36 ± 0.02	0.18 ± 0.02	$0.08 \pm {}^{+0.17}_{-0.05}$
γ	[km s^{-1}]	1.246 ± 0.001	-40.267 ± 0.001	$-21.858 \pm {}^{+0.008}_{-0.005}$
ω	[°]	202.7 ± 3.1	232.5 ± 9.4	$98 \pm {}^{+92}_{-51}$
K_1	[m s^{-1}]	34.9 ± 0.8	36.4 ± 1.2	$71 \pm {}^{+18}_{-8}$
$f(m)$	[10^{-9} $M_\odot$]	1.37 ± 0.10	4.94 ± 0.50	16.4 ± 12.6
$a_1 \sin i$	[10^{-3} AU]	1.15 ± 0.03	3.42 ± 0.12	2.95 ± 0.75
$m_2 \sin i$	[$M_{\rm Jup}$]	1.16 ± 0.03	1.90 ± 0.06	3.09 ± 0.79
a	[AU]	1.03 ± 0.03	2.07 ± 0.06	1.25 ± 0.04
N		29	21	26
$\sigma_{\rm O-C}$ ♮	[m s^{-1}]	1.7	1.6	8.5
$\chi^2_{\rm red}$ ⋆		1.45	1.46	26.7
$p(\chi^2, \nu)$ ‡		0.074	0.11	0

† JD = BJD − 2 453 000. ♮ $\sigma_{\rm O-C}$ is the weighted rms of the residuals (weighted by $1/\epsilon^2$, where ϵ is the O−C uncertainty). ⋆ $\chi^2_{\rm red} = \chi^2/\nu$ where ν is the number of degrees of freedom (here $\nu = N - 6$). ‡ Post-fit χ^2 probability computed with $\nu = N - 6$.

3. HARPS radial-velocity data

Stars belonging to the volume-limited HARPS-GTO subprogramme are observed most of the time without the simultaneous thorium-argon reference (Baranne et al. 1996). The obtained radial velocities are thus uncorrected for possible instrumental drifts. This only has a very low impact on our results as the HARPS radial-velocity drift is less than 1 m s^{-1} over one night. For this large volume-limited sample, we aim at a radial-velocity precision of the order of 3 m s^{-1} (or better). This corresponds roughly to an SNR of 40−50 at 5500 Å. For bright targets like the three stars of this paper, the exposure times required for reaching this signal level can be very short as an SNR of 100 (at 5500 Å) is obtained with HARPS in a 1-min exposure on a 6.5 mag G dwarf under normal weather and seeing conditions. In order to limit the impact of observing overheads (telescope preset, target acquisition, detector read-out), we normally do not use exposure times less than 60 s. As a consequence, the SNR obtained for bright stars is significantly higher than the targeted one, and the output measurement errors are frequently below 2 m s^{-1}.

For our radial-velocity measurements, we consider two main error terms. The first one is obtained through the HARPS Data Reduction Software (DRS). It includes all the known calibration errors ($\simeq$20 cm s^{-1}), the stellar photon-noise, and the error on the instrument drift. For observations taken with the simultaneous reference, the drift error is derived from the photon noise of the thorium-argon exposure. For observations taken without the lamp, a drift error term of 50 cm s^{-1} is quadratically added. The second main error term is called the non-photonic error. It includes guiding errors and a lower limit for the stellar pulsation signals. For the volume-limited programme, we use an ad-hoc value for this term: 1.0 m s^{-1}. Stellar noise (activity jitter, pulsation signal) can of course be greater in some cases (as for example for HD 221287, cf. Sect. 3.3). The non-photonic term nearly vanishes for targets belonging to the very high RV precision sample (non-active stars, pulsation modes averaged out by the specific observing strategy). In this latter case, this term thus only contains the guiding errors: $\simeq$30 cm s^{-1}. The error bars listed in this paper correspond to the quadratic sum of the DRS and the non-photonic errors.

In the following sections, we present the HARPS radial-velocity data obtained for HD 100777, HD 190647, and HD 221287 in more detail, as well as the orbital solutions fitted to the data.

3.1. A 1.16 $M_{\rm Jup}$ planet around HD 100777

We have gathered 29 HARPS radial-velocity measurements of HD 100777. These data span 858 days between February 27th 2004 (BJD = 2 453 063) and July 4th 2006 (BJD = 2 453 921). Their mean radial-velocity uncertainty is 1.6 m s^{-1} (mean DRS error: 1.3 m s^{-1}). We list these measurements in Table 2 (electronic version only).

A nearly yearly signal is present in these data. We fitted a Keplerian orbit. The resulting parameters are listed in Table 5. The fitted orbit is displayed in Fig. 1, together with our radial-velocity measurements. The radial-velocity data is best explained by the presence of a 1.16 $M_{\rm Jup}$ planet on a 384 d fairly eccentric orbit (e = 0.36). The inferred separation between the host star and its planet is a = 1.03 AU. Both $m_2 \sin i$ and a were computed using a primary mass of 1 $M_\odot$.

We performed Monte-Carlo simulations using the *ORBIT* software (see Sect. 3.1 in Forveille et al. 1999) in order to double-check the parameter uncertainties. The errorbars obtained from these simulations are quasi-symmetric and somewhat larger ($\simeq$18%) than the ones obtained from the covariance matrix of the Keplerian fit. The errors we have finally quoted in Table 5 are the Monte-Carlo ones. The residuals to the fitted orbit (see bottom panel of Fig. 1) are flat and have a dispersion compatible with the measurement noise. The low reduced χ^2 value (1.45) and the χ^2 probability (0.074) further demonstrate the good fit quality. The presence of another massive short-period companion around HD 100777 is thus unlikely.

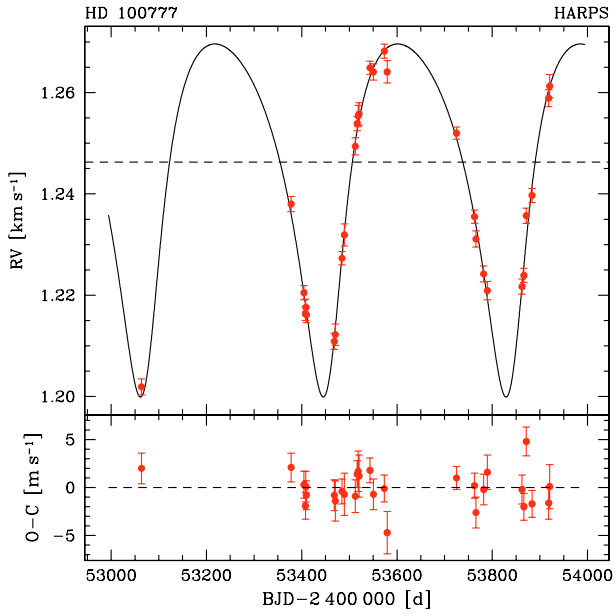

Fig. 1. *Top*: HARPS radial-velocity data (dots) for HD 100777 and fitted orbital solution (solid curve). The radial-velocity signal is induced by the presence of a 1.16 $M_{\rm Jup}$ planetary companion on a 384-day orbit. *Bottom*: residuals to the fitted orbit. The scatter of these residuals is compatible with the velocity uncertainties.

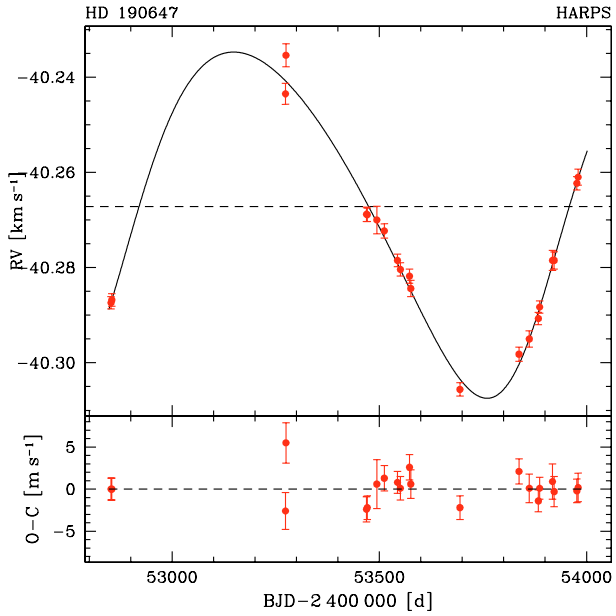

Fig. 2. *Top*: HARPS radial-velocity data (dots) for HD 190647 and fitted orbital solution (solid curve). The radial-velocity signal is induced by the presence of a 1.9 $M_{\rm Jup}$ planetary companion on a 1038-day orbit. *Bottom*: residuals to the fitted orbit. The scatter of these residuals is compatible with the velocity uncertainties.

3.2. A 1.9 $M_{\rm Jup}$ planet orbiting HD 190647

Between August 1, 2003 (BJD = 2 452 852) and September 2, 2006 (BJD = 2 453 980), we obtained 21 HARPS radial-velocity measurements for HD 190647. These data have a mean radial-velocity uncertainty of 1.7 m s^{-1} (mean DRS error: 1.3 m s^{-1}). We list these measurements in Table 3 (electronic version only).

A long-period signal is clearly present in the RV data. We performed a Keplerian fit. The resulting fitted parameters are listed in Table 5. The fitted orbital period (1038 d) is slightly shorter than the observing time span (1128 d) and the orbital eccentricity is low (0.18). Monte-Carlo simulations were carried out. The uncertainties on the orbital parameters obtained in this case are nearly symmetric and a bit larger (≃18%) than the ones resulting from the Keplerian fit. In Table 5, we have listed these more conservative Monte-Carlo uncertainties. The small discrepancy between the two sets of errorbars is most probably due to the rather short time span of the observations (only 1.09 orbital cycle covered) and to our still not optimal coverage of both the minimum and the maximum of the radial-velocity orbit. From the fitted parameters and with a primary mass of 1.1 $M_\odot$, we compute a minimum mass of 1.90 $M_{\rm Jup}$ for this planetary companion. The computed separation between the two bodies is 2.07 AU. Figure 2 shows our data and the fitted orbit.

The weighted rms of the residuals (1.6 m s^{-1}) is slightly smaller than the mean RV uncertainty. The low dispersion of the residuals, the low reduced χ^2 value, and its associated probability (0.11) allow us to exclude the presence of an additional massive short-period companion.

3.3. A 3.1 $M_{\rm Jup}$ planetary companion to HD 221287

A total of 26 HARPS radial-velocity data were obtained for HD 221287. These data are spread over 1130 days: between July 31, 2003 (BJD = 2 452 851) and September 3, 2006 (BJD = 2 453 981). Unlike the two other targets presented in this paper, a substantial fraction (≃65%) of these velocities were taken using the simultaneous thorium-argon reference. They were thus corrected for the measured instrumental velocity drifts. The mean radial-velocity uncertainty computed for this data set is 2.1 m s^{-1} (mean DRS error: 1.8 m s^{-1}). We list these measurements in Table 4 (electronic version only).

A 456 d radial-velocity variation is clearly visible in our data (see Fig. 3). This period is two orders of magnitude longer than the rotation period obtained from the Noyes et al. (1984) calibration for HD 221287: 5 ± 2 d. This large discrepancy between $P_{\rm RV}$ and $P_{\rm rot}$ is probably sufficient for safely excluding stellar spots as the origin of the detected RV signal, but we nevertheless checked if this variability could be due to line-profile variations. The cross-correlation function (CCF) bisector span versus radial velocity plot is shown in the top panel of Fig. 4. The average CCF bisector value is computed in two selected regions: near the top of the CCF (i.e. near the continuum) and near its bottom (i.e. near the RV minimum). The span is the difference between these two average values (top−bottom) and thus represents the overall slope of the CCF bisector (for details, see Queloz et al. 2001).

As for the case of HD 166435 presented in Queloz et al. (2001), an anti-correlation between spans and velocities is expected in the case of star-spot induced line-profile variations. The bisector span data are quite noisy (weighted rms of 10.4 m s^{-1}), but they are not correlated with the RV data. The main signal can therefore not be due to line-profile variations and certainly has a Keplerian origin.

Table 5 contains the results of a Keplerian fit that we performed. Our data and the fitted orbit are displayed in Fig. 3. The RV maximum remains poorly covered by our observations. As for the other two targets, we made Monte-Carlo simulations for checking our orbital parameter uncertainties. As expected, the uncertainties obtained in this case largely differ from the ones obtained via the Keplerian fit. For most of the parameters, the errorbars resulting from the simulations are not symmetric and much larger (≃5 times larger). In order to be more conservative, we have chosen to quote these errors in Table 5.

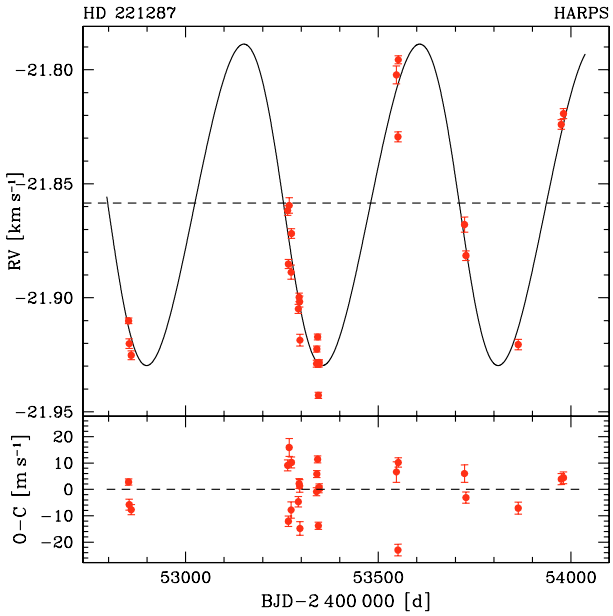

Fig. 3. *Top*: HARPS radial-velocity data (dots) for HD 221287 and fitted orbital solution (solid curve). The detected Keplerian signal is induced by a 3.1 $M_{\rm Jup}$ planet on a 456-day orbit. Because of a non-optimal coverage of the radial-velocity maximum and the presence of stellar activity-induced jitter, the exact shape of the orbit is not very well-constrained. *Bottom*: residuals to the fitted orbit. The scatter of these residuals is much larger than the velocity uncertainties. This large dispersion is probably due to the fairly high activity level of this star.

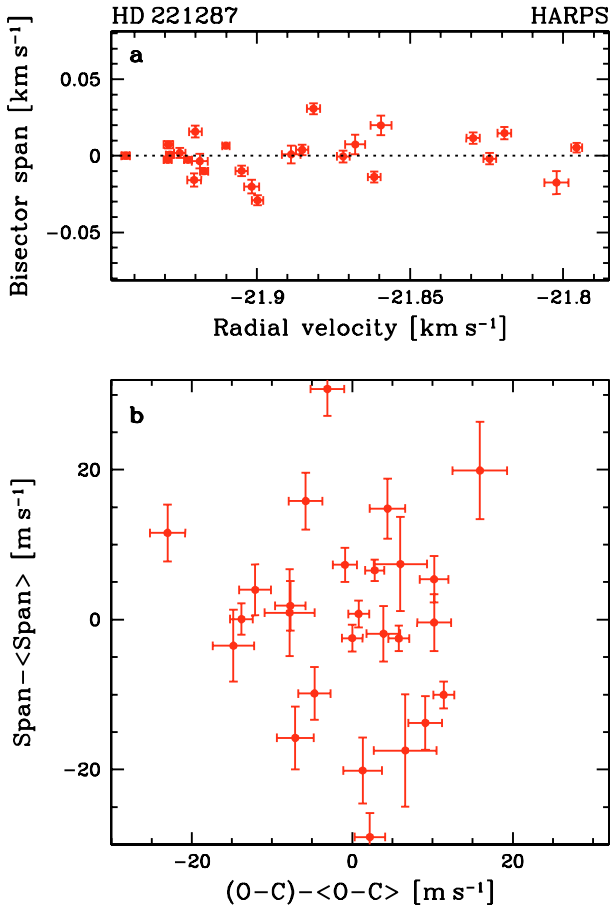

Fig. 4. a) Bisector span versus radial-velocity plot for HD 221287. The dispersion of the span data is quite large (10.4 m s^{-1}) revealing potential line-profile variations. Nevertheless, the main radial-velocity signal is not correlated to these profile variations and is thus certainly of Keplerian origin. **b)** Bisector span versus radial-velocity residuals to the Keplerian orbit (see Table 5) displayed in the same velocity scale. A marginal anti-correlation between the two quantities is observed.

The shape of the orbit is not very well-constrained, but there is no doubt about the planetary nature of HD 221287 b. The fitted eccentricity is low (0.08), but circular or moderately eccentric orbits (up to 0.25) cannot be excluded yet. Using a primary mass of 1.25 $M_{\odot}$, we compute the companion minimum mass and separation: $m_2 \sin i = 3.09\ M_{\rm Jup}$ and $a = 1.25$ AU.

3.4. Residuals to the HD 221287 orbital fit

The residuals to the orbital solution for HD 221287 presented in Sect. 3.3 are clearly abnormal. Their weighted rms, 8.5 m s^{-1}, is much larger than the mean radial-velocity uncertainty obtained for this target: $\langle \epsilon_{RV} \rangle = 2.1$ m s^{-1}. The abnormal scatter obtained by quadratically correcting the residual rms for $\langle \epsilon_{\rm RV} \rangle$ is 8.2 m s^{-1}. This matches the lowest value expected for this star from the Santos et al. (2000) and Wright (2005) studies. Again, we stress that these two studies clearly lack active F stars, and their activity versus jitter relations are thus weakly constrained for this kind of target. Our measured jitter value certainly does not strongly disagree with their results.

We have searched for periodic signals in the radial-velocity residuals by computing their Fourier transform, but no significant peak in the power spectrum could be found. The absence of significant periodicity is not surprising since the phase of star-spot induced signals is not always conserved over more than a few rotational cycles.

Cross-correlation function bisector spans are plotted against the observed radial-velocity residuals in the bottom panel of Fig. 4. A marginal anti-correlation (Spearman's rank correlation coefficient: $\rho = -0.1$) between the two quantities is visible. A weighted linear regression (i.e the simplest possible model) was computed. The obtained slope is only weakly significant (1σ). We are thus unable, at this stage, to clearly establish the link between the line-profile variations and our residuals. As indicated in Sect. 3.3, our orbital solution is not very well-constrained. This probably affects the residuals and possibly explains the absence of a clear anti-correlation. Additional radial-velocity measurements are necessary for establishing this relation, but activity-related processes so far remain the best explanation for the observed abnormal residuals to the fitted orbit.

HD 221287 has a planet with an orbital period of 456 d but with an additional radial-velocity signal, probably induced by the presence of cool spots whose visibility is modulated by stellar rotation.

4. Conclusion

We have presented our HARPS radial-velocity data for 3 Solar-type stars: HD 100777, HD 190647, and HD 221287. The radial-velocity variations detected for these stars are explained by the presence of planetary companions. HD 100777 b has a minimum mass of 1.16 $M_{\rm Jup}$. Its orbit is eccentric (0.36) and has a period of 384 days. The 1038-day orbit of the 1.9 $M_{\rm Jup}$ planet around the slightly evolved star HD 190647 is moderately eccentric (0.18).

The planetary companion inducing the detected velocity signal for HD 221287 has a minimum mass of $3.1\,M_{\rm Jup}$. Its orbit has a period of 456 days. The orbital eccentricity for this planet is not well-constrained. The fitted value is 0.08 but orbits with $0.0 \leq e \leq 0.25$ cannot be excluded yet. This rather weak constraint on the orbital shape is explained by two reasons. First, our data cover the radial-velocity maximum poorly. Second, the residuals to this orbit are abnormally large. We have tried to establish the relation between these high residuals and line-profile variations through a study of the CCF bisectors. As expected, a marginal anti-correlation of the two quantities is observed, but it is only weakly significant, thereby preventing us from clearly establishing the link between them.

Acknowledgements. The authors would like to thank the ESO–La Silla Observatory Science Operations team for its efficient support during the observations and to all the ESO staff involved in the HARPS maintenance and technical support. Support from the Fundação para Ciência e a Tecnologia (Portugal) to N.C.S. in the form of a scholarship (reference SFRH/BPD/8116/2002) and a grant (reference POCI/CTEAST/56453/2004) is gratefully acknowledged. Continuous support from the Swiss National Science Foundation is appreciatively acknowledged. This research has made use of the Simbad database operated at the CDS, Strasbourg, France.

References

Baranne, A., Queloz, D., Mayor, M., et al. 1996, A&AS, 119, 373
Benz, W., & Mayor, M. 1981, A&A, 93, 235
ESA 1997, The HIPPARCOS and TYCHO catalogue, ESA-SP 1200
Flower, P. J. 1996, ApJ, 469, 355
Forveille, T., Beuzit, J., Delfosse, X., et al. 1999, A&A, 351, 619
Girardi, L., Bressan, A., Bertelli, G., & Chiosi, C. 2000, A&AS, 141, 371
Israelian, G., Santos, N. C., Mayor, M., & Rebolo, R. 2004, A&A, 414, 601
Lo Curto, G., Mayor, M., Clausen, J. V., et al. 2006, A&A, 451, 345
Lovis, C., Mayor, M., Pepe, F., et al. 2006, Nature, 441, 305
Mayor, M., Pepe, F., Queloz, D., et al. 2003, The Messenger, 114, 20
Moutou, C., Mayor, M., Bouchy, F., et al. 2005, A&A, 439, 367
Noyes, R. W., Hartmann, L. W., Baliunas, S. L., Duncan, D. K., & Vaughan, A. H. 1984, ApJ, 279, 763
Pace, G., & Pasquini, L. 2004, A&A, 426, 1021
Pepe, F., Mayor, M., Queloz, D., et al. 2004, A&A, 423, 385
Pepe, F., Mayor, M., Rupprecht, G., et al. 2002, The Messenger, 110, 9
Queloz, D., Henry, G. W., Sivan, J. P., et al. 2001, A&A, 379, 279
Santos, N. C., Mayor, M., Naef, D., et al. 2000, A&A, 361, 265
Santos, N. C., Mayor, M., Naef, D., et al. 2002, A&A, 392, 215
Santos, N. C., Bouchy, F., Mayor, M., et al. 2004a, A&A, 426, L19
Santos, N. C., Israelian, G., & Mayor, M. 2004b, A&A, 415, 1153
Schaerer, D., Meynet, G., Maeder, A., & Schaller, G. 1993, A&AS, 98, 523
Schaller, G., Schaerer, D., Meynet, G., & Maeder, A. 1992, A&AS, 96, 269
Sestito, P., & Randich, S. 2005, A&A, 442, 615
Udry, S., Mayor, M., Naef, D., et al. 2000, A&A, 356, 590
Wright, J. T. 2005, PASP, 117, 657

Online Material

Table 2. HARPS radial-velocity data obtained for HD 100777.

Julian date BJD – 2 400 000 [d]	*RV* [km s^{-1}]	Uncertainty [km s^{-1}]
53 063.7383	1.2019	0.0016
53 377.8740	1.2380	0.0015
53 404.7626	1.2205	0.0014
53 407.7461	1.2164	0.0014
53 408.7419	1.2176	0.0016
53 409.7891	1.2161	0.0015
53 468.6026	1.2109	0.0016
53 470.6603	1.2122	0.0021
53 484.6703	1.2273	0.0013
53 489.5948	1.2319	0.0022
53 512.5671	1.2494	0.0017
53 516.5839	1.2539	0.0014
53 518.5962	1.2554	0.0021
53 520.5778	1.2558	0.0022
53 543.5598	1.2649	0.0013
53 550.5289	1.2641	0.0016
53 573.4689	1.2682	0.0014
53 579.4705	1.2641	0.0022
53 724.8617	1.2520	0.0012
53 762.8169	1.2355	0.0013
53 765.7645	1.2311	0.0016
53 781.8894	1.2242	0.0016
53 789.7730	1.2209	0.0018
53 862.6200	1.2217	0.0015
53 866.6037	1.2239	0.0014
53 871.6270	1.2357	0.0015
53 883.5589	1.2397	0.0014
53 918.4979	1.2589	0.0017
53 920.5110	1.2613	0.0023

Table 3. HARPS radial-velocity data obtained for HD 190647.

Julian date BJD – 2 400 000 [d]	*RV* [km s^{-1}]	Uncertainty [km s^{-1}]
52 852.6233	−40.2874	0.0013
52 854.6727	−40.2868	0.0013
53 273.5925	−40.2435	0.0022
53 274.6041	−40.2354	0.0024
53 468.8874	−40.2688	0.0015
53 470.8634	−40.2689	0.0014
53 493.9234	−40.2700	0.0029
53 511.9022	−40.2723	0.0015
53 543.8020	−40.2785	0.0013
53 550.7721	−40.2804	0.0014
53 572.8074	−40.2818	0.0015
53 575.7266	−40.2844	0.0017
53 694.5136	−40.3056	0.0014
53 836.9226	−40.2982	0.0015
53 861.8630	−40.2950	0.0017
53 883.8224	−40.2907	0.0013
53 886.8881	−40.2883	0.0013
53 917.8390	−40.2785	0.0021
53 921.8472	−40.2785	0.0018
53 976.6039	−40.2623	0.0014
53 979.6654	−40.2610	0.0017

Table 4. HARPS radial-velocity data obtained for HD 221287.

Julian date BJD – 2 400 000 [d]	*RV* [km s^{-1}]	Uncertainty [km s^{-1}]
52 851.8534	−21.9101	0.0012
52 853.8544	−21.9201	0.0021
52 858.7810	−21.9252	0.0019
53 264.7097	−21.8617	0.0021
53 266.6805	−21.8852	0.0020
53 268.7030	−21.8595	0.0034
53 273.6951	−21.8888	0.0031
53 274.7129	−21.8718	0.0021
53 292.6284	−21.9049	0.0020
53 294.6239	−21.8998	0.0019
53 295.6781	−21.9017	0.0024
53 296.6388	−21.9186	0.0026
53 339.6009	−21.9289	0.0015
53 340.5974	−21.9225	0.0013
53 342.5955	−21.9172	0.0013
53 344.5961	−21.9428	0.0014
53 345.5923	−21.9291	0.0013
53 346.5566	−21.9284	0.0013
53 546.9385	−21.8022	0.0039
53 550.9121	−21.8294	0.0022
53 551.9479	−21.7956	0.0018
53 723.5707	−21.8679	0.0033
53 727.5302	−21.8815	0.0021
53 862.9297	−21.9205	0.0023
53 974.7327	−21.8240	0.0021
53 980.7273	−21.8192	0.0022